26. M. J. Cieslak, in *Metal Science of Joining*, M. J. Cieslak, J. H. Perepezko, S. Kang, M. E. Glicksman, Eds. (TMS, Warrendale, PA, 1991), p. 101.
27. K. W. Mahin *et al.*, in *Recent Trends in Welding Science and Technology*, S. A. David and J. M. Vitek, Eds. (ASM International, Materials Park, OH, 1990), p. 83.
28. M. C. Flemings, *Solidification Processing* (McGraw-Hill, New York, 1974); J. F. Matsuda, T. Hashimoto, T. Senda, *Trans. Natl. Res. Inst. Met. (Jpn.)* **11(1)**, 83 (1969); W. F. Savage, *Weld. World* **18**, 89 (1980); K. E. Easterling, *Introduction to Physical Metallurgy of Welding* (Butterworth, London, 1983), p. 48.
29. R. Mehrabian, *Int. Metall. Rev.* **27**, 185 (1982); J. M. Vitek, A. DasGupta, S. A. David, *Metall. Trans.* **14A**, 1833 (1983); S. A. David, J. M. Vitek, T. L. Hebble, *Weld J. (Miami, Fla.)* **66**, 289s (1987); S. Katayama and A. Matsunawa, *Proceedings of the International Congress on Application of Lasers and Electro-optics* (Laser Institute of America, Boston, 1984), vol. 44, pp. 60–67; J. W. Elmer, S. M. Allen, T. W. Eagar, *Metall. Trans.* **20A**, 2117 (1989).
30. R. Trivedi and W. Kurz, *Acta Metall.* **34**, 1663 (1986); W. J. Boettinger and S. R. Coriell, *Mater. Sci. Eng.* **65**, 27 (1984); M. J. Aziz, *J. Appl. Phys.* **53**, 1158 (1982).
31. J. A. Brooks and M. I. Baskes, in *Advances in Welding Science and Technology*, S. A. David, Ed. (ASM International, Materials Park, OH, 1987), p. 93; J. C. Lippold and W. F. Savage, in *Modeling of Casting and Welding Processes*, H. D. Brody and D. Apelian, Eds. (Metallurgical Society of AIME, Warrendale, PA, 1980), p. 443.
32. W. F. Savage, C. D. Lundin, A. Aronson, *Weld. J. (Miami, Fla.)* **44**, 175s (1965).
33. S. A. David and C. T. Liu, *ibid.* **61**, 157s (1982).
34. M. Rappaz, S. A. David, J. M. Vitek, L. A. Boatner, *Metall. Trans.* **21A**, 1767 (1990); S. A. David, J. M. Vitek, M. Rappaz, L. A. Boatner, *ibid.*, p. 1753.
35. H. W. Kerr and J. C. Villafuerte, in *Metal Science of Joining*, M. J. Cieslak, J. H. Perepezko, S. Kang, M. E. Glicksman, Eds. (TMS, Warrendale, PA, 1991), p. 11.
36. J. M. Vitek and S. A. David, *Weld. J. (Miami, Fla.)* **63**, 246s (1984); *ibid.* **67**, 95s (1988); S. A. David, J. M. Vitek, J. R. Keiser, W. C. Oliver, *ibid.* **66**, 235s (1987), C. F. Willis, R. Gromsky, T. M. Divine, *Metall. Trans.* **22A**, 2889 (1991).
37. D. L. Olson, in *Recent Trends in Welding Science and Technology*, S. A. David and J. M. Vitek, Eds. (ASM International, Materials Park, OH, 1990), p. 553.
38. G. E. Cook, K. Andersen, R. J. Barrett, in *ibid.*, p. 891.
39. H. B. Smartt and J. A. Johnson, in *Proceedings of the Artificial Neural Networks in Engineering (ANNIE '91)*, St. Louis, MO, 10 to 13 November 1991, C. H. Dagli, S. R. T. Kumara, Y. C. Shin, Eds. (ASME, New York, 1991), p. 711
40. L. J. Jones, J. H. Lang, T. W. Eagar, paper presented at the 3rd International Conference on Trends in Welding Research, Gatlinburg, TN, 1 to 5 June 1992 (AMS International, Materials Park, OH)
41 H M. Hale and D. E. Hardt, *ibid.*
42 R. W Richardson, A. Gutow, R. A. Anderson, D F. Farson, *Weld. J (Miami, Fla.)* **63**, 43s (1984).
43. J. Bolstad, *Proceedings of the Advances in Automation for Precision Arc Welding*, Columbus, OH, 2 to 3 December 1987 (Edison Welding Institute, Columbus, OH, 1987).
44. B. A. Chin, N. H. Madsen, J. S. Goodlng, *Weld. J. (Miami, Fla.)* **62**, 227s (1983); S. Nagarajan, P. Banerjee, W. Chen, B A. Chin, *IEEE Trans. Robot. Autom.* **8(1)**, 1 (1991).
45. Supported by the Division of Materials Sciences, the U.S. Department of Energy, under contract DE-AC05-84OR21400 with Martin Marietta Energy Systems, Inc., and grant DE-FGO2-84ER45158 with the Pennsylvania State University. Helpful comments from M. M Coleman, W. M. Small, P. A. Thrower, W. A. Yarbrough, E. P. George, and C T. Liu are gratefully acknowledged.

RESEARCH ARTICLE

Three-Dimensional Structure of an Angiotensin II–Fab Complex at 3 Å: Hormone Recognition by an Anti-Idiotypic Antibody

K. Christopher Garcia,* Pierre M. Ronco, Pierre J. Verroust, Axel T. Brünger, L. Mario Amzel†

The elucidation of bioactive conformations of small peptide hormones remains an elusive goal to structural chemists because of the inherent flexibility of these molecules. Angiotensin II (AII), the major effector of the renin-angiotensin system, is an octapeptide hormone for which no clear structural models exist. Peptide hormones such as AII share the property that they bind to their receptors with high affinities, in spite of the fact that they must overcome an extremely large conformational entropy barrier to bind in one conformation. A "surrogate system" that consists of a high-affinity monoclonal antibody (MAb) and AII has been used to study a bound conformation of AII. The crystallographic structure of the complex reveals a structure of AII that is compatible with predicted bioactive conformations of AII derived from structure-activity studies and theoretical calculations. In the complex, the deeply bound hormone is folded into a compact structure in which two turns bring the amino and carboxyl termini close together. The antibody of this complex (MAb 131) has the unusual property that it was not generated against AII, but rather against an anti-idiotypic antibody reactive with a MAb to AII, which renders this antibody an anti–anti-idiotypic antibody. The high affinity for AII of the original MAb to AII was passed on to MAb 131 through a structural determinant on the anti-idiotypic antibody. Strikingly, the conformation of AII in this complex is highly similar to complementarity determining region loops of antibodies, possibly indicating that a true molecular mimic of bound AII was present on the anti-idiotypic antibody against which MAb 131 was elicited.

Angiotensin II (AII) is the primary active component of the renin-angiotensin system and plays a central role in the regulation of blood pressure. The hormone, an octapeptide of sequence Asp-Arg-Val-Tyr-Ile-His-Pro-Phe, participates in a number of physiological functions associated with the regulation of blood pressure. Receptors for AII have been identified in blood vessels, heart, liver, adrenal gland, and pituitary gland, where they mediate vasoconstriction, ionotropic effects, glycogenolysis, secretion of aldosterone, and release of prolactin, respectively (*1*). Direct effects of AII on the central nervous system have also been described (*2*).

The renin-angiotensin system has been the target of extensive drug design efforts for control of hypertension. Inhibitors of angiotensin-converting enzyme—mechanism-based inhibitors of the cleavage of the inactive pro-decapeptide angiotensin I (AI) to AII—are some of the most successful antihypertensive drugs (*3*). Yet, the most effective inhibitor of AII action would be a molecule that directly prevents the binding of AII to its receptor. Unfortunately, success in designing molecules that act as AII receptor antagonists has been hindered by the lack of direct structural information concerning the bioactive conformation of AII.

Angiotensin II has been the subject of extensive study to determine its solution conformation or conformations; however, its extreme flexibility has hindered attempts at determining its structure by either spectroscopic or crystallographic methods (*4*).

K. C Garcia and L. M Amzel are in the Department of Biophysics and Biophysical Chemistry, Johns Hopkins University School of Medicine, Baltimore, MD 21205. P. M. Ronco and P J. Verroust are in the INSERM Unité 64, Hôpital Tenon, Paris 75790 Cedex 20, France.
A. T. Brunger is in the Howard Hughes Medical Institute and Department of Molecular Biophysics and Biochemistry, Yale University, New Haven, CT 06511.
*Present address: Departments of Molecular Biology and Protein Engineering, Genentech, Inc., South San Francisco, CA 94080.
†To whom correspondence should be addressed.

In addition, recent data on cyclosporin A and FK506 indicate that their solution conformations bear little resemblance to their receptor-bound conformations (*5*, *6*). These results have dramatically reemphasized the importance of knowing the conformation of the bound state for the understanding of biological function and for the design of bioactive analogs (*7*). The recently cloned AII receptors are integral membrane proteins of the multiple transmembrane helix class, as are many receptors for small (<20 residues) peptide hormones (*8*). Angiotensin II is a prototype for these extremely flexible peptide hormones (such as substance K, vasopressin, and bradykinin) whose receptors are intractable to study by crystallography (at the present time) yet whose bound conformations are of critical pharmacological importance. One way to obtain structural information about these peptide hormones is to study the structure of complexes of the hormones with high-affinity monoclonal antibodies (MAb's). In this article, we describe the three-dimensional structure of such a complex between the Fab fragment of MAb 131 and AII.

Antibodies have been produced against AII and have been used by several groups to gain insight into the properties of the hormone and its receptor or receptors (*9*). Most MAb's appear to be directed against the carboxyl-terminal region of the AII peptide—the same region that is most important in hormonal activity and most sensitive to amino acid substitutions. Most of these MAb's also bind AII analogs, and in some cases their affinities for the analogs parallel the bioactivity of the compounds. Furthermore, an anti-idiotypic antibody against one of these monoclonals was shown to bind the AII receptor (*10*). These observations lend credence to the idea that an antibody can be used as a "surrogate receptor" for biophysical studies of the bound state of the peptide.

The structure of the antibody described in this article (MAb 131) contains an additional level of information relevant to understanding recognition of flexible molecules. MAb 131 is an anti–anti-idiotypic antibody (Ab3) that recognizes AII with high affinity and specificity even though it was raised against an anti-idiotypic antibody (Ab2) rather than AII itself (*11*).

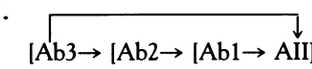

All of the experimental evidence in this system suggests that the anti-idiotypic antibodies (Ab2) have the characteristics expected from an "internal image"–bearing antibody: they appear to display an image of AII that elicits AII-reactive Ab3 (*12*). Thus MAb 131 is a rare example of an antibody to a globular protein that is able to bind a small peptide with high affinity. The structure of the complex presented here not only provides a conformation of AII bound with high affinity but also has information for understanding anti-idiotypic recognition phenomena and for developing drug design strategies aimed at scaffolding bioactive peptides into large proteins.

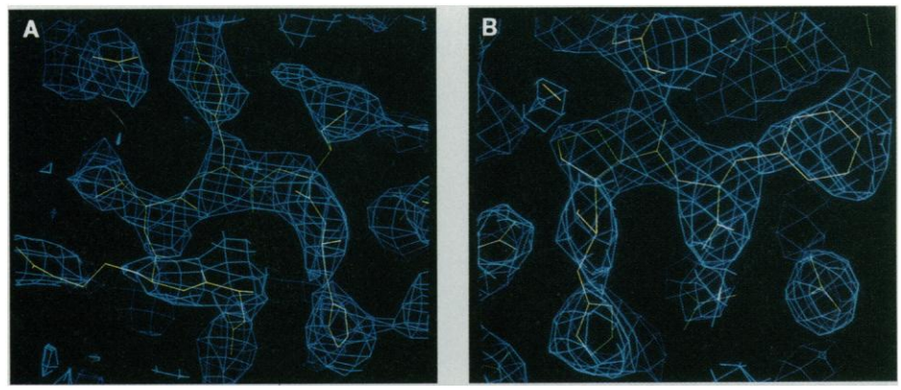

Fig. 1. The $2F_o - F_c$ omit electron density map of bound AII. A 12 Å sphere around the peptide was omitted from structure factor calculations for a round of simulated annealing (2000 to 300 K) and positional refinement. The compact fold of the peptide requires that it be shown in two planar projections so that all of the electron density can be seen. (**A**) and (**B**) are related by a 90° rotation around the axis of His^6 parallel to the vertical plane of the page. In (A) (showing residues Asp^1-Arg^2-Val^3-Tyr^4-Ile^5-His^6), the residues of (B) (His^6-Pro^7-Phe^8) point directly out of the page. Map display was made on an Evans and Sutherland PS390 by using the graphics program FRODO; contouring is at 1.1 σ. Methods: Cocrystals were grown from PEG-300, 0.1 M sodium acetate with a molar ratio of hormone to Fab of 2:1 [presence of the peptide in the crystal was verified as described (*13*)]. Data from two crystals were collected on a Siemens multiwire area detector and were processed and merged with the program Xengen (*32*). The final R_{merge} for 26,500 reflections collected out of 34,000 possible (78 percent complete to 2.8 Å) was 0.125 {$R_{merge} = \Sigma\Sigma|I_j(h) - \langle(h)\rangle|/[\Sigma\Sigma\, I_j(h)]$; summations were done over all reflections in all crystals}. Data were weak past 3.0 Å, as reflected in the R_{merge}, because of rapid radiation decay.

Structure determination. We have reported two related crystal forms of Fab 131 (*13*). The A form was crystallized from polyethylene glycol 400 (PEG-400), 0.1 M imidazole, pH 7.4, and is space group $P4_3$, with cell dimensions $a = b = 78.6$ Å and $c = 124.0$ Å. This form, obtained with the unliganded Fab, diffracts to 4.0 Å and has one molecule in the asymmetric unit (collected 8600 out of 9200 possible reflections). The B form, which contains the Fab-AII complex, was crystallized from PEG-300, 0.1 M sodium acetate, pH 4.75, diffracts to 2.8 Å resolution, and has two molecules in the asymmetric unit (collected 26,500 out of 34,000 possible reflections). The B form is also space group $P4_3$ but has cell dimensions $a = b = 110.0$ Å and $c = 124.0$ Å. The cell dimensions of the two forms are related by the following transformation: $a_B \approx \sqrt{2}a_A$; $c_B \approx c_A$. The B form appears to be related to the A form by a lattice transformation involving a slight distortion of the molecules of the A form at every other lattice point. This results in new reflections in the B form such that the new reflections (those with $h + k$ = odd) are mostly weak. Knowledge of this transformation allowed us to determine the structure of the B form analytically from the solution of the A form.

The structure of Fab 131 was determined by molecular replacement using both the Crowther rotation function as implemented in the package MERLOT (*14*) and the Patterson correlation (PC) refinement method of XPLOR (*15*). The native, lower resolution A form was solved first because it had fewer molecules in the asymmetric unit. A common solution was found with four of seven search models by using the Crowther rotation function, but further progress was hampered by an ambiguity concerning the number of molecules in the asymmetric unit. The PC refinement, as implemented in XPLOR, in which HyHEL-5 (*16*) was used as the search model, indicated a clear solution and the presence of only one molecule in the asymmetric unit for the A form crystal. One round of simulated annealing refinement lowered the R factor from 0.42 to 0.28 [$R = (\Sigma|F_o - F_c|)/\Sigma|F_o|$, where F_o and F_c are the observed and calculated structure factors, respectively]. This model was then used to solve the B form by the appropriate coordinate transformation and placement of two Fab molecules at (0.0, 0.0, 0.0) and (0.5, 0.5, 0.0). Rigid-body refinement followed by simulated annealing (*17*) lowered the R factor from 0.45 to 0.30 for the B form data (20,000 reflections with $I/\sigma > 1.6$). At this point the amino acid sequence for the variable (V) region of Fab 131 became available and was built into the $2F_o - F_c$ omit maps where each complementarity determining

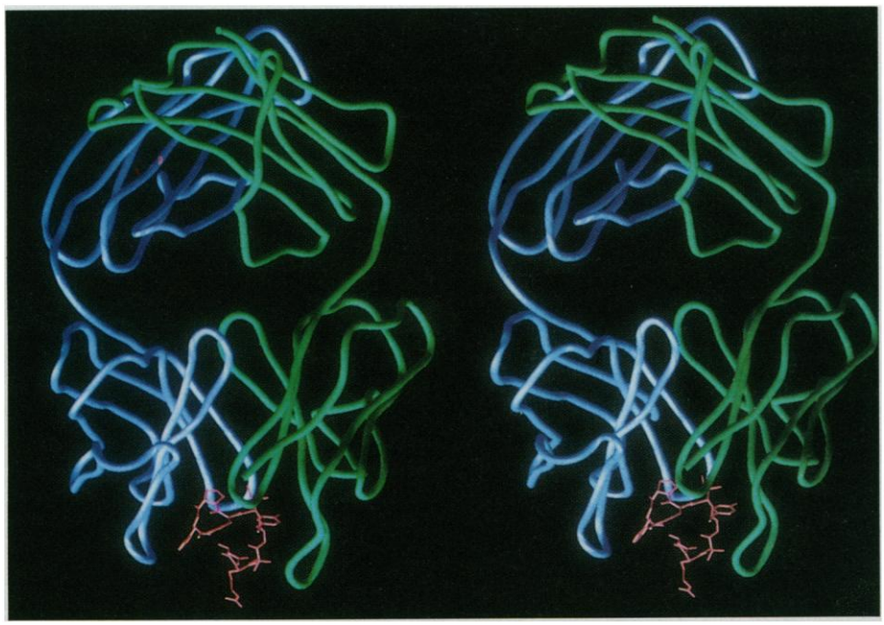

Fig. 2. Stereoview of the Fab 131–AII complex. Heavy chain is in blue, light chain is in green, and the peptide is in red. Shown is one of the two molecules in the asymmetric unit. Display generated by program RIBBONS (*33*) on an Iris Silicon Graphics workstation.

Table 1. Buried surface area breakdown of the complex by CDR (*31*). Residues of Fab 131 that are part of the buried surface area are in boldface, and the residues that are the largest contributors to the buried surface area are in underlined boldface. (Not all of the residues in van der Waals contact have large contributions to the buried surface area.) Surface area values were calculated by the program MS as implemented into a package by S. Sheriff. The total buried surface area for Fab 131 is 725 Å^2 and for AII is 620 Å^2. The corresponding breakdown for the residues in AII (in percent) is Asp^1, 7; Arg^2, 6; Val^3, 6; Tyr^4, 21; Ile^5, 15; His^6, 12; Pro^7, 12; and Phe^8, 21.

	Chain and sequence	Buried surface area (percent)
	25 31a b c d e f	
L1	**S S Q N L L <u>H</u> S I T R K N Y**	27
	50 56	
L2	**W A S T R G S**	0
	89 95	
L3	**K Q S Y N L <u>Y</u>**	14
	30 35	
H1	**N T D A M N**	7
	50 52a b c 53	
H2	**<u>R</u> I R S K G <u>F</u> N F A T Y Y A D**	21
	96 105	
H3	**V R G <u>R</u> D G E A M D**	29

region (CDR) was, in turn, omitted from the structure factor calculations for a round of positional refinement and manual fitting. The starting model of the constant domain was that of HyHEL-5. Further rounds of simulated annealing and rebuilding lowered the *R* factor to 0.27. Each molecule was built independently, and noncrystallographic symmetry constraints were not applied during the refinement. The five carboxyl-terminal residues of the light chain (residues 218 to 222 of the constant region) do not have interpretable electron density and are not included in the final model. The peptide was not built into the density until after the combining site had been satisfactorily refined.

In both molecules of the complex, the peptide electron density is found inside the cleft formed by the long CDR's L1 (light chain) and H2 (heavy chain) and adjacent to CDR H3. The peptide was fitted into a simulated annealing $2F_o - F_c$ omit map where all residues of the model within 12 Å of the peptide density had been omitted (Fig. 1). There was clear density in both Fab molecules for the residues Val^3 through Phe^8, and these were easily built in. The amino-terminal Asp^1 and Arg^2 protrude from the combining site and have density that is less well defined than the rest of the peptide. In one of the two molecules, however, the density is adequate to allow unambiguous fitting. The electron density of Ile^5 of the peptide is well defined in one of the two molecules, whereas in the other molecule this density is poor (shown in Fig. 1). Further rounds of simulated annealing and positional refinement and individual isotropic *B*-factor refinement lowered the *R* factor to 0.25 (20,000 reflections > 1.6 σ). The root-mean-square (rms) deviation from ideality for bond lengths is 0.025 Å, for bond angles is 4.7°, and for planarity of the peptide bond is 2.7°.

Since each molecule in the asymmetric unit was refined independently, a rigorous test for the accuracy of the model is the rms deviation between the coordinates of the two molecules. Both molecules, considering their relation in the unit cell and the relation between the A and the B crystal form, should be almost identical. The rms deviation between the α-carbon atoms of framework residues of the two Fab molecules is 0.79 Å for the variable domain of the light chains (VL) and 0.74 Å for the variable domain of the heavy chains (VH). The rms deviation for the constant domains is 0.8 Å for both light and heavy chains. The rms deviation between the two peptides in each Fab molecule is 0.7 Å. Considering that the mean coordinate error for this structure, derived from a Luzatti plot, is 0.3 to 0.4 Å, the two molecules in the unit cell are essentially identical (*18*). The lower resolution of the A form data does not allow us to make any comparisons between the liganded and unliganded Fab's.

Structure description. The Fab 131 complex contains the immunoglobulin fold found in all antibody molecules (Fig. 2). The elbow angle of both molecules of Fab 131 is 151.7°, in the middle of the range of values found in other Fab structures. The V region has very long CDR's, especially L1 and H3. The loops formed by CDR's L1 and H2 protrude from the combining site and form a very deep cleft between them; the long CDR H3 runs in the middle of the cleft and folds back, forming a flat floor for the combining site. The external portions of CDR's H3 and L3 form the sides of the narrow portion of the cleft; deep in the cavity, in the region contiguous to the framework residues, they make extensive van der Waals contacts and hydrogen bonds with each other. The resulting combining site is lined with many aromatic residues (especially Tyr) but it has also a high proportion of polar residues (especially Arg and Ser).

Angiotensin II is bound deep inside the cleft formed by the long CDR's; it is tightly packed against CDR H3, which forms a wall behind the peptide at the back of the cavity. In this position, the peptide is centered around the pseudo twofold axis relating VH and VL with a small offset (1 to 2 Å) toward the heavy chain (also seen in Fig. 2).

The bound AII has a very compact conformation containing two turns (Figs. 3 and 4). The main turn, with respect to determining the mode of binding, consists of a tight turn involving residues Ile^5, His^6, and Pro^7; the center of this turn is lodged in the deepest region of the combining site. The other major turn involves Asp^1 and Arg^2. The effect of this turn is to bring the amino terminus of the peptide back toward the combining site in such a way that the

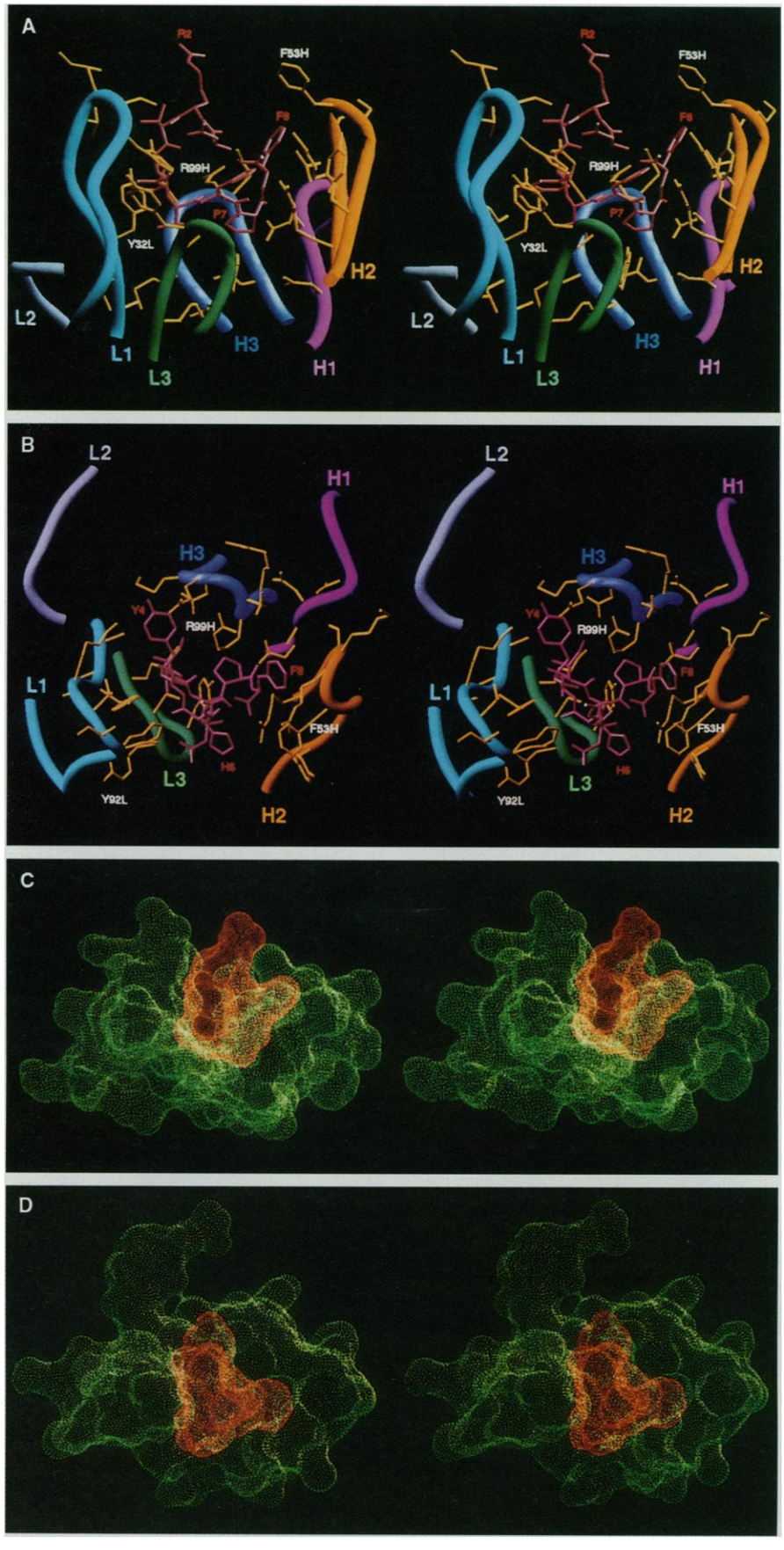

Fig. 3. Stereo views of the combining site of the Fab 131–AII complex. (**A**) Side view and (**B**) front view (looking directly into the combining site) showing AII (in red), all six CDR main chains, and the side chains of the CDR residues within van der Waals contact of the peptide (in yellow). The main chains of the CDR's are shown in different colors and are labeled L1, L2, L3, H1, H2, and H3. (**C** and **D**) Identical orientations as (A) and (B), respectively, but only the van der Waals dot surface is shown. The peptide is in red, and the Fab combining site is in green. The van der Waals surface was calculated by the program MS with a 1.7 Å probe and displayed using the program RIBBONS (*33*).

amino and carboxyl termini of the peptide are in close spatial proximity. This conformation appears to involve a salt bridge between the termini and a hydrogen bond between the side chain of Asp^1 and the main-chain carbonyl of His^6.

Peptide-protein interactions. The extent of the interaction between the Fab and the peptide was evaluated by calculating the loss of exposed surface area upon the formation of the complex. The buried surface area, calculated with the program MS (*19*) with a 1.7 Å probe radius and standard van der Waals radii (*20*), indicated a high degree of surface complementarity between the bound antigen and the antibody. Upon complex formation, 725 $Å^2$ of the Fab become buried together with 620 $Å^2$ of the peptide. There are slight differences (±6 percent) in the values of the buried surface areas of the hormone between the two molecules because of the coordinate error expected in a 3 Å structure. Approximately 22 CDR residues contribute to the overall buried surface area (Table 1). A breakdown of the contributions of the CDR's of the light and heavy chains shows a preferential interaction of the peptide with the heavy chain. Although the peptide is bound along the pseudo twofold axis relating VL and VH, almost two-thirds of the contacts involve the heavy chain. Four CDR's, L1, L3, H2, and H3, make extensive contacts with the peptide and account for 91 percent of the total buried area; H1 contributes only 7 percent and L2 does not contact the peptide at all. [Other antigen-antibody complexes also have interactions dominated by the heavy chain, and L2 is frequently not in contact with antigen (*20*).] The major contributors to the buried surface area are His^{L31}, Tyr^{L95}, Arg^{H50}, Arg^{H52}, and Phe^{H53}; the largest contributor is Arg^{H99}.

Fourteen CDR residues are involved in van der Waals contacts with the peptide (Table 2 and Figs. 3 and 4). Diverse types of interactions stabilize the complex with a slight predominance of hydrophobic contacts; contacts include many van der Waals interactions, hydrogen bonds, and a salt

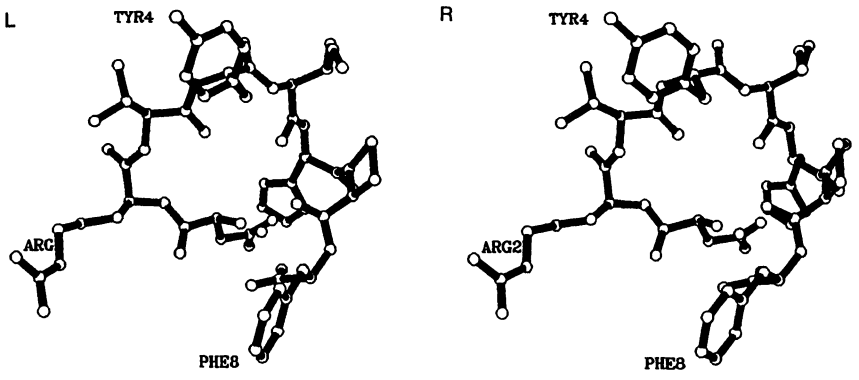

Fig. 4. Stereo view of the peptide alone; Fab residues not shown. Drawing plotted by program PLUTO.

Table 2. Residues of the peptide-Fab complex that are within van der Waals contact distance (4.1 Å) of each other.

Angiotensin II	Fab 131
Asp^1	His^{L31}, Ser^{L31a}
Arg^2	Ser^{L31a}
Val^3	None
Tyr^4	His^{L31}, Lys^{L31e}, Tyr^{L32}, Arg^{H99}, Glu^{H102}
Ile^5	Tyr^{L32}
His^6	Ser^{L91}, Tyr^{L95}, Arg^{H52}
Pro^7	Tyr^{L92}, Ala^{H33}, Arg^{H52}, Arg^{H99}
Phe^8	Arg^{H50}, Arg^{H52}, Phe^{H53}, Gly^{H52c}, Arg^{H99}

bridge. The most crucial interactions involve residues from CDR H3; Arg^{H99} has extensive polar and nonpolar contacts with both the side chains and the main chain of the peptide. [The involvement of Arg residues of antibodies in extensive hydrophobic interactions is discussed in Mian *et al.* (*21*).] His^6 of the peptide is close to Tyr^{L92}, Asn^{H36}, and Tyr^{H59}. There are a number of contacts that are close enough to be possible hydrogen bonds: the NH of Arg^2 of the peptide is 3.1 Å away from the Nδ of His^{L31}, the NH of His^6 is 2.9 Å from the Oγ of Ser^{L91} and its Nε is 3.0 Å from the Nη of Arg^{H50}, and the carboxyl-terminal carboxylate is 3.5 Å from the Nη Arg^{H52} and the Nη Arg^{H50}. The side chain of Asp^1 is centered in a region that contains the guanidinium groups of two Arg residues, Arg^{H50} and Arg^{H52} (the Nη of Arg^{H50} is 4.3 Å of the Oδ of Asp^1 of the peptide). (Small differences exist between the two complexes in the asymmetric unit.)

Angiotensin II antagonists and anti-idiotypic networks. The association constant K_a of AII for Fab 131 ($7.4 \times 10^9\ M^{-1}$) is one of the largest association constants of all of the antibody-antigen complexes of known structure and is almost two orders of magnitude tighter than the other published peptide-Fab complexes solved crystallographically (*22*). The buried surface area in these complexes varies over a wide range, from 500 $Å^2$ for the moderate affinity Fab-peptide complex (*22*) to greater than 800 $Å^2$ for the Fab-neuroaminidase complex (*20*). The extent of buried surface area for the formation of the Fab 131–AII complex, which corresponds to burying the large concave surface of the binding site groove, is 725 $Å^2$ for the Fab and 620 $Å^2$ for the peptide and is comparable to the area buried in the complexes of antibodies with large globular proteins. As in the case of globular proteins, ~60 percent of the buried surface area is hydrophobic and ~40 percent is polar. The recently solved crystal structure of HLA-B2 with peptide shows a buried molecular surface area for the complex of 1200 $Å^2$ for the HLA and 800 $Å^2$ for the peptide (*23*). Extensive surface complementarity appears to correlate with high binding affinity.

The structure reported here provides a simple and direct rationale for the high affinity of the antibody for the flexible peptide. The binding site of the antibody is very deep and narrow. This has two effects: (i) it markedly increases the exposed surface area of the free antibody and (ii) it creates a volume from which it is easy to exclude solvent by simply filling the cavity. The peptide folds into a compact structure that fills the cavity so exactly that in the complex the bound peptide forms a contiguous convex surface with the rest of the protein, completely obliterating the deep cavity. Burying this large surface can partially account for the high affinity of MAb 131 for AII. The release of solvent bound to the cavity can compensate for the large conformational entropy loss suffered by the peptide upon binding.

The experimental data concerning the specificity of MAb 131 for AII are consistent with the structure of the complex reported here (*9*, *11*). As measured by competition ELISA (enzyme-linked immunosorbent assay), MAb 131, like almost all antibodies to AII, is primarily specific for the six carboxyl-terminal residues. Deletions and substitutions in the amino-terminal residues are well tolerated: only a moderate loss of affinity results from deletion of the amino-terminal Asp^1 and Arg^2, and the Asp can be replaced by sarcosine while retaining full binding activity. In the structure, the Asp^1 and Arg^2 are the least buried, most solvent-exposed residues of the peptide. The most buried residues are part of the central AII sequence -Tyr^4-Ile^5-His^6-Pro^7-, which is also the most immunogenic epitope of the peptide (*9*). Most substitutions of these immunogenic residues abolish binding to MAb 131. The only exception, the substitution of Ile^5 to Val, can be explained with the structure of the complex: Ile^5 is in van der Waals contact with only one residue of the Fab. Phe^8 of the hormone is also very sensitive to substitutions, not only for binding to this antibody but also for binding to the natural AII receptor. The location of the Phe^8 of the peptide in the complex provides a good explanation for the observation that AI, which has two additional residues on the carboxyl terminus, binds MAb 131, but with a two to three order of magnitude reduction in affinity. In the complex, the Phe^8 is near enough to the outside of the combining site that the additional residues of AI could extend out of the binding site into the solvent, yet the carboxyl terminus of the AII peptide is buried enough that some distortions of the peptide, and maybe also the Fab, would be necessary to accommodate the extension.

The central immunodominant residues of AII occur in the most deeply buried portion of the peptide in the complex; they are also the most important residues in binding of AII to its receptor. This fact is a good first indication that the structure of the Fab-bound hormone is relevant to the bioactive conformation. Further evidence can be found in the striking congruence between the structure of the Fab-bound AII and existing models for the bioactive conformation of the hormone based on spectroscopic studies of AII in solution and structure-activity studies of peptide and nonpeptide analogs. Spectroscopic studies (nuclear magnetic resonance, circular dichroism, and fluorescence energy transfer) have indicated a rapid conformational equilibrium between highly solvated and folded structures (*4*). Nevertheless, there have been several models proposed for the most stable solution conformations of AII (*24*, *25*). Although the models differ in detail, they all have characteristics in common with the conformation of AII in the Fab 131–AII complex. They predict that AII exhibits two turns: one turn involves the Pro^7 and the other involves the amino-

terminal Asp-Arg-Val-Tyr. These two turns bring the amino and carboxyl termini into close proximity, folding AII into a compact structure. These models, as well as the Fab-bound conformation of AII, are supported by structure-activity studies, which indicate that rigidification of AII analogs into one or more turns by methods such as D-amino acid incorporation, cyclization, and isosteric peptide bonds can yield high-affinity receptor antagonists.

Recently, a number of very tightly binding nonpeptide AII antagonists have been developed by using the AII model of Fermandjian and co-workers, which also proposes that an interaction between the amino and carboxyl termini compacts the peptide into a turn (*26*). These nonpeptide antagonists were designed to mimic the close spatial disposition of Tyr^4, Pro^7, and Phe^8 of AII in this folded model. The basic design of the molecules (imidazole-5-acrylic acids) is a central imidazole ring (to represent Pro^7) with thienyl (to mimic Phe^8) and benzoate (Tyr^4) groups orthogonal to each other. The structure of the Fab 131–bound AII exhibits a roughly similar spatial disposition of these residues. Manual alignment of this drug with the AII conformation in the complex (using the logic of the design strategy) showed that the imidazole aligned with the Pro^7, the thienyl overlapped with the Phe^8, and the Tyr^4 needed to be rotated by 80° around the Cα–Cβ bond toward the center of the turn to overlap it with the benzoate ring of the drug.

Angiotensin II has been shown to bind Ca^{2+} at submillimolar concentrations (*27*). Lenkinski and Glickson took advantage of the Ca^{2+}-binding properties of AII: they substituted the Ca^{2+} by the paramagnetic metal Gd^{3+} to measure Gd^{3+}-induced proton relaxation rates of the hormone (*24*). The addition of Gd^{3+} resulted in the disappearance of the CαH resonances of Asp^1 and Phe^8 together with severe line broadening of the corresponding resonances of Arg^2, Val^3, and Pro^7. The resonances of Tyr^4, Ile^5, and His^6 remain relatively sharp, indicating that they are furthest away from the metal. The model resulting from these studies had the β-carboxylate of Asp and the carboxyl-terminal carboxylate coordinated to the Gd^{3+}, giving the peptide backbone a **C** shape. The structure proposed by these authors has many features similar to those of the Fab 131–bound model of the peptide. Angiotensin II may be a case, then, in which there is coincidence between a low-energy solution structure and the bound conformation.

The compactness of the structure of the bound peptide, as well as the similarity of the values of buried surface area to those of Fab complexes of antibodies to globular proteins, can be correlated with the anti–anti-idiotypic properties of MAb 131. The peptide structure could have been the part of the "internal image–bearing" Ab2 that bore the "image" of AII and elicited MAb 131 (*28*). [For example, one CDR loop with a conformation similar to that of the bound AII could have been present in the Ab2.] To probe this point further, we carried out a search of the crystallographic database that indicated that the peptide structure found in the complex bore a high conformational similarity to the CDR3 loop of the human antibody light chain dimer REI (*29*), yielding an rms distance between the backbones of 0.80 Å for the aligned residues (residues 2 through 8 of AII aligned to residues 90 to 96 of REI). Thus it seems possible that the mimic of the hormone in the Ab2 is a single CDR loop. If this is the case, the conformation of the flexible hormone is faithfully presented by the Ab2, which has favorable implications for strategies for the improvement of the half-lives of peptide-based drugs by grafting the peptides into proteolytically stable globular proteins. Humanization of antibodies has emerged as an important method of targeting anticancer drugs to specific tissues and cells in humans (*30*). Because AII structure was presented in an accessible manner by the Ab2, it might be possible to deliver hormone activities of small peptides (agonists or antagonists) in the form of a humanized anti-idiotypic antibody.

REFERENCES AND NOTES

1. J. H. Laragah and J. Sealy, *Handb. Physiol.* **8**, 831 (1973).
2. M. I. Phillips, *Neuroendocrinology* **25**, 354 (1978).
3. P. Corvol, *Clin. Exp. Hypertens. Part A Theory Pract.* **11**, 463 (1989).
4. R. W. Woody, in *Conformation in Biology and Drug Design*, V. J. Hruby, Ed., vol. 7 of *The Peptides* (Academic Press, Orlando, FL, 1985), pp. 15–114.
5. C. Weber *et al.*, *Biochemistry* **30**, 6563 (1991); S. W. Fesik *et al.*, *ibid.*, p. 6574; K. Wüthrich *et al.*, *Science* **254**, 953 (1991).
6. G. D. Van Duyne, R. F. Standaert, P. A. Karplus, S. L. Schreiber, J. Clardy, *Science* **252**, 839 (1991); S. W. Michnick, M. K. Rosen, T. J. Wandless, M. Karplus, S. L. Schreiber, *ibid.*, p. 836; J. M. Moore, D. A. Peattie, M. J. Fitzgibbon, J. A. Thomson, *Nature* **351**, 248 (1991).
7. W. L. Jorgensen, *Science* **254**, 954 (1991).
8. K. Sasaki *et al.*, *Nature* **351**, 230 (1991); T. J. Murphy, R. W. Alexander, K. K. Griendling, M. S. Runge, K. E. Bernstein, *ibid.*, p. 233.
9. P. O. J. Couraud, *J. Immunol.* **136**, 3365 (1986); M. Budisavljevic *et al.*, *ibid.* **140**, 3059 (1988); M. B. Valloton, *Handb. Exp. Pharmacol.* **37**, 185 (1974)
10. P. O. J. Couraud, *J. Immunol.* **138**, 1164 (1987).
11. M. Budisavljevic, P. M. Ronco, P. J. Verroust, *ibid.* **145**, 1440 (1990).
12. N. K. Jerne, *Ann. Immunol. (Inst. Pasteur)* **125**, 373 (1974); A. Nisonoff and E. Lamoyi, *Clin. Immunol. Immunopathol.* **21**, 397 (1981).
13. K. C Garcia, P. Ronco, P. J. Verroust, L. M. Amzel, *J. Biol. Chem.* **264**, 20463 (1989).
14. P. M. D. Fitzgerald, *J. Appl. Crystallogr.* **21**, 273 (1988).
15. A. T. Brünger, *Acta Crystallogr. Sect. A* **46**, 46 (1990).
16. S. Sheriff *et al.*, *Proc. Natl. Acad. Sci. U.S.A.* **84**, 8075 (1987).
17. A. T. Brunger, *XPLOR Manual Version 2.1* (Yale University, New Haven, CT, 1990).
18. P. V. Luzatti, *Acta Crystallogr.* **5**, 802 (1952).
19. M. L. Connoly, *J. Appl. Crystallogr* **16**, 548 (1983).
20. D. R. Davies, E. A. Padlan, S. Sheriff, *Annu. Rev. Biochem.* **59**, 439 (1990).
21. I. S. Mian, A. R. Bradwell, A. J. Olson, *J. Mol. Biol.* **217**, 133 (1991).
22. R. L. Stanfield, T. M. Fieser, R. A. Lerner, I. A. Wilson, *Science* **248**, 712 (1990); J. M. Rini, U. Schulze-Gahmen, I. A. Wilson, *ibid.* **255**, 959 (1992).
23. D. R. Madden, J. C. Gorga, J. L. Strominger, D. C. Wiley, *Nature* **353**, 321 (1991).
24. R. E. Lenkinski and J. D. Glickson, in *Conformation in Biology and Drug Design*, V. J. Hruby, Ed., vol. 7 of *The Peptides* (Academic Press, Orlando, FL, 1985), pp. 301–354.
25. A. Aumelas *et al.*, *Proc. Natl. Acad. Sci. U.S.A.* **82**, 1881 (1985); C. R. Marshall, H. E. Bosshard, W. H. Vine, J. D. Glickson, P. Needleman, in *Recent Advances in Renal Physiology and Pharmacology*, L. G. Wesson and G. M. Farelli, Eds. (Johns Hopkins Univ. Press, Baltimore, MD, 1974), pp. 215–256.
26. J. Weinstock *et al.*, *J. Med. Chem.* **34**, 1514 (1991).
27. R. E. Lenkinski and R. L. Stephens, *J. Inorg. Biochem.* **15**, 95 (1981).
28. K. C. Garcia, S. J. Desideiro, P. M. Ronco, P. J. Verroust, L. M. Amzel, *Science* **257**, 528 (1992).
29. D. Epp *et al.*, *Eur. J. Biochem.* **45**, 513 (1979).
30. L. Reichmann, M. Clark, H. Waldmann, G. Winter, *Nature* **332**, 327 (1988).
31. Abbreviations for the amino acid residues are: A, Ala; C, Cys; D, Asp; E, Glu; F, Phe; G, Gly; H, His; I, Ile; K, Lys; L, Leu; M, Met; N, Asn; P, Pro; Q, Gln; R, Arg; S, Ser; T, Thr; V, Val; W, Trp; and Y, Tyr.
32. A. J. Howard *et al.*, *J. Appl. Crystallogr.* **20**, 383 (1987).
33. M. Carson, personal communication.

34. Supported by NIH grant GM44692. K.C.G. is a predoctoral fellow of the IBRMA supported by the NSF. We thank M. Carson (University of Alabama) for the use of the program RIBBONS.

30 March 1992; accepted 18 June 1992